Phase-locked arrays of surface-emitting terahertz quantum-cascade lasers

Tsung-Yu Kao,[1,a)] Qing Hu,[1] and John L. Reno[2]
[1]*Department of Electrical Engineering and Computer Science, Research Laboratory of Electronics, Massachusetts Institute of Technology, Cambridge, Massachusetts 02139, USA*
[2]*Department 1123, Sandia National Laboratories, MS 0601, Albuquerque, New Mexico 87185-0601, USA*

(Received 11 January 2010; accepted 16 February 2010; published online 10 March 2010)

We report the demonstration of phase-locked arrays of surface-emitting distributed-feedback (DFB) terahertz quantum-cascade lasers with single-mode operations. Carefully designed "phase sector" locks several surface-emitting DFB laser ridges in-phase, creating tighter beam-patterns along the phased-array direction with full width at half maximum (FWHM) $\approx 10°$. In addition, the phase sector can be individually biased to provide a mechanism of frequency tuning through gain-induced optical index change, without significantly affecting the output power levels. A tuning range of 1.5 GHz around 3.9 THz was achieved. This fine tunability could be utilized to frequency- or phase-lock the DFB array to an external reference. © *2010 American Institute of Physics*.
[doi:10.1063/1.3358134]

The best terahertz (THz) quantum-cascade lasers (QCLs) in terms of high-temperature operation have been demonstrated based on the metal-metal (MM) waveguides,[1,2] which provide strong mode confinement and low waveguide losses. However, the subwavelength confinement in the vertical dimension results in divergent beam-patterns.[3] The second-order surface-emitting distributed feedback (DFB) laser[4,5] improves the far-field beam-patterns while preserving the benefit of MM waveguide; but due to the asymmetric dimension of light emitting area, the beam-pattern is tighter along the grating direction and much broader in the cross direction. In order to expand the coherent light emitting areas in both directions, approaches such as two-dimensional photonic-crystal structures on MM waveguides,[6,7] and integrated horn antennas[8] have been developed. An ingenious solution for a tight and symmetric beam pattern was developed recently based on a third-order DFB structure.[9] In this letter, we present another method of generating symmetric beam patterns by using phase-locked arrays of second-order DFB lasers. The physical separation of the DFB laser ridges reduces the average power dissipation per effective light emitting area, which is advantageous for continuous wave (*cw*) operations. Different DFB laser ridges in the array are coupled through carefully designed phase sectors. Each laser ridge is engineered to be locked in-phase with each other. This phase-locked laser array has tighter beam-patterns along the array-direction, which is orthogonal to the DFB grating direction. Furthermore, independent bias of the phase sector produces a fast and fine frequency tuning for frequency- or phase-lock the array to an external reference.

In order to phase-lock all elements in an array, there are four coupling schemes in integrated diode laser systems—laser ridges are coupled through exponentially decaying fields outside the high index dielectric core (evanescent-wave coupled[10]) or through the Talbot feedback from external reflectors (diffraction-wave coupled[11]) or by connecting two ridges to one single-mode waveguide (Y-coupled[12]) or through lateral propagating waves (leaky-wave coupled[13]). Among these coupling schemes, leaky-wave coupled devices show the most robust operation.[14] The evanescent-wave coupled scheme suffers several disadvantages. First, due to the decaying nature of evanescent waves, couplings beyond nearest neighbors are negligible, leading to poor modal discrimination between adjacent modes. Besides, evanescent-wave coupled devices tend to favor out-of-phase mode and therefore it is not ideal for single-lobe operations.[15] The diffraction-wave coupled scheme generally relies on external optical feedbacks. For a MM waveguide with 50 μm width, the reflectivity of a facet at THz can be $\sim$90%,[16] which makes sufficient feedbacks challenging. Y-coupled schemes have been demonstrated in mid-infrared QCLs,[17] but in general, these devices show undesirable self-pulsation dynamics between in-phase and out-of-phase modes[18] due to spatial hole burning effect.

In order to incorporate the leaky-wave coupled scheme, couplings between laser ridges must occur through propagating waves, which, for MM waveguides, does not exist in the lateral direction. A solution to that is as following: consider two identical DFB lasers which lase at the same frequency but with arbitrary phase relations. When connecting these two lasers through a phase sector in series, standing waves will form inside the phase sector and force the phase relation between the two lasers to be either 0 or π. The proposed laser arrays consist of two parts—DFB laser ridges and phase sectors. A series of apertures are opened on the top metal of the DFB ridges to form second-order gratings. A π shifter is implemented in the center of the grating to achieve single-lobe beam-patterns along the DFB direction. Tapered ends are used to connect the DFB ridges and the phase sectors (with a narrower width) in order to ensure single-lateral-mode operations across the whole array. The DFB laser ridges and phase sectors are electronically isolated by gaps on the top and side metals.

Figure 1(b) shows the surface losses versus eigenfrequencies of the fundamental lateral modes from a finite-element three-dimensional simulation of a three-ridge surface-emitting DFB array. By choosing a proper phase sector length, the desired in-phase mode will have the lowest surface loss and therefore will be the lasing mode. The transverse magnetic fields for the in-phase, out-of-phase, and ad-

a)Electronic mail: wilt_kao@mit.edu.

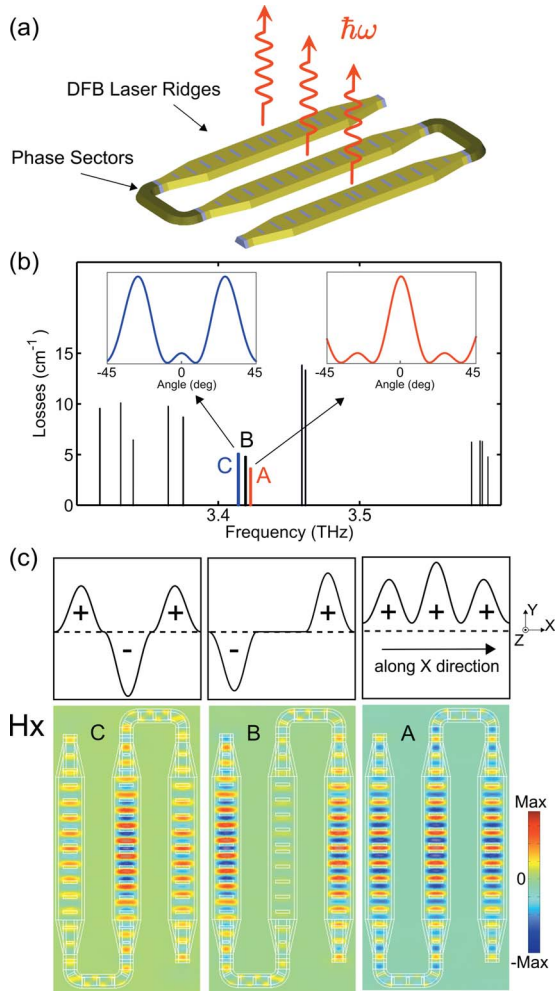

FIG. 1. (Color online) (a) Diagram of a three-ridge surface-emitting DFB array. (b) Computed surface losses vs eigenfrequencies from three-dimensional finite-element method simulations on the same array. For the particular length of the phase sector used in the simulation, the in-phase mode (a) has the lowest surface loss. Adjacent mode (b) and out-of-phase mode (c) are also labeled. The insets show the far-field beam-patterns along the array direction for in-phase and out-of-phase modes. (c) Computed transverse magnetic fields for different spatial modes and their corresponding H-field magnitude diagrams along x direction.

jacent modes are shown on Fig. 1(c). The in-phase mode has single-lobe, while out-of-phase mode has dual-lobe far-field beam-patterns along the array direction [shown in the insets in Fig. 1(b)]. The proper length (s) of the phase sector is determined by the so called "*resonance condition*" in Ref. 14,

$$s = m\frac{\lambda_{ps}}{2}, \tag{1}$$

where λ_{ps} is the wavelength along the propagating direction inside the phase sector and m is an integer number. The laser array is operated in the in-phase/out-of-phase mode when m is odd/even.

The THz QCL gain medium, labeled as FL183S grown by molecular-beam epitaxy (wafer VA0094) was first Cu–Cu thermal bonded with a n^+ GaAs receptor wafer, annealed, and substrate-removed to expose the 10 μm thick QCL structure. The highly doped top contact layer was then etched away. The grating was defined by using image reversal photoresist AZ5214 and a lift-off process (Ta/Au, 25/350 nm).

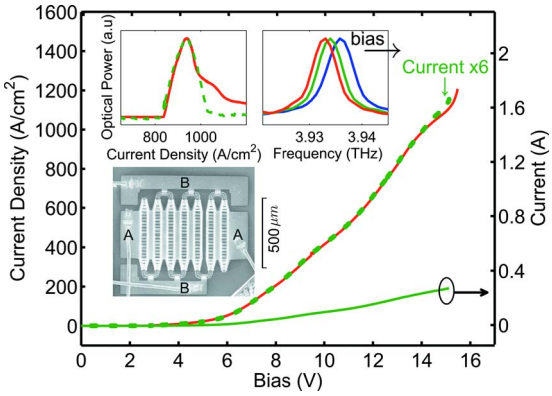

FIG. 2. (Color online) Pulsed I-V curves from a single ridge DFB laser (solid line, near bottom) and a six-ridge DFB array (solid line, near top). The scaled I-V curve of the single-ridge device (dotted line) is also shown. The J_{th} of six-ridge device is 815 A/cm^2 as compared with 810 A/cm^2 of the single-ridge device. The emission spectra from the six-ridge device are single-mode at all biases. The scanning electron microscope (SEM) picture of a similar array device is also shown in the inset. The main laser ridges and the phase sectors have different bonding pads (labeled as A and B in the picture, respectively).

To obtain outward sloped sidewalls for biasing the laser ridge from the side, the same special wet-etching techniques described in Ref. 4 was used to define laser ridges and phase sectors. A 300-nm-thick SiO_2 was blanketedly deposited as the electric isolation layer, followed by a buffered oxide etch to open the top of ridges. The bonding pad and the metal on sidewalls were defined by another lift-off process (Ta/Au, 25/500 nm) using negative photoresist NR71–3000P (Futurrex, Inc.). The wafer was further lapped down and the bottom electric contact (Ta/Au 25/250 nm) was deposited. The devices were then cleaved, die sawed into smaller subchips, In/Au die-bonded to a copper chip carrier, wire bonded, and then mounted to a pulsed tube cryorefrigerator, where the L-I-V characterizes of the devices were measured at a temperature of 10 K in pulse mode using a He-cooled Ge:Ga photodetector. Unfortunately, due to contamination in metal layers, the lasing threshold of the DFB devices (J_{th}) increased to ~800 from 550 A/cm^2 of simple Fabry–Perot devices fabricated using similar wet etching. As a result, the highest pulsed operation temperature is only ~30 K, and no *cw* operation can be achieved with the DFB arrays.

Figure 2 shows pulsed I-V curves from a single ridge DFB laser and an array of six ridges. The scaled I-V curve of single ridge device matches well with the measurement from a six-ridge DFB array, indicating the uniformity of devices and bias conditions. The L-I measurements in the inset also show similar behaviors for both devices. The device emits ≈1 mW pulsed power at 10 K. The length of individual ridge is ~500 μm and the distance between adjacent ridges is 100 μm.

Figure 3 shows the measured far-field beam-patterns along the array direction (x-direction) for different laser arrays. It is clear that all array devices show phase-locking behaviors. Both double-ridge arrays have identical laser ridges but different phase sectors lengths [different m numbers in Eq. (1)]. They emit at almost identical frequency but are locked in different spatial modes. This demonstrates that the laser array can be operated in either in-phase or out-of-phase mode by choosing different *resonance conditions* which is a signature of leaky-wave coupled scheme. The

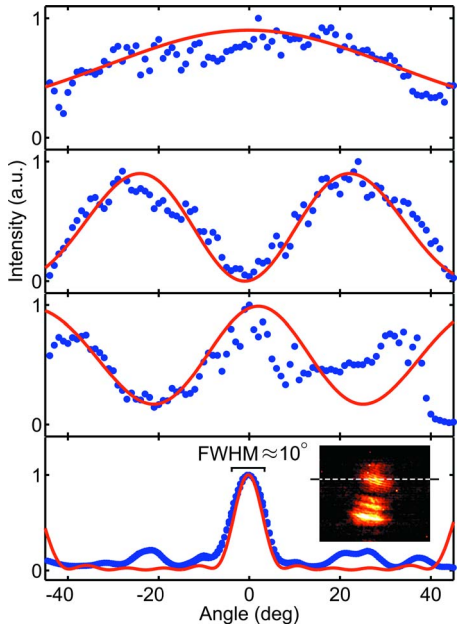

FIG. 3. (Color online) Far-field (20 cm) beam-patterns along array direction (x) (solid circles) and simple point source simulation using measured emission frequencies ($\sim$127.5 cm^{-1}) and the distance (100 μm) between ridges (solid line) for different laser arrays. For single-ridge device, the simulated curve is the diffraction pattern of a single slit with the width of ridge. From top to bottom: single-ridge laser, a double-ridge array operated in the out-of-phase mode, another double-ridge array operated in the in-phase mode, and the six-ridge array (as shown in Fig. 2). The THz emission image from the six-ridge array taken by the microbolometer camera used in Ref. 19 is shown in the inset. The one-dimensional beam-pattern was measured along the dotted line.

six-ridge array is operated in the in-phase mode and its far-field beam-pattern shows a single central lobe with FWHM $\approx 10°$, which agrees well with the simulation. Due to a fabrication error, the π shifter was implemented too small and thus failed to achieve the desired single-lobe beam-patterns along the DFB direction (y-direction). Even though these devices showed dual-lobe beam-patterns in the DFB direction (y), it does not affect the working principle of the phase sectors and also the demonstration of phase-locking along the array direction (x).

In addition, the phase sector can be individually biased to provide another frequency tuning mechanism through gain-induced optical index change, without significantly affecting the output power levels. For a gain medium with 60 cm^{-1} peak gain at 3.8 and 1 THz Lorentzian linewidth, about 0.4%–0.6% change in optical index can be achieved, assuming 10% of field energy resides in the phase sector. This will induce $\sim$0.05% change in frequency (corresponding to $\sim$1.9 GHz). Figure 4 shows the measured frequency shift in the emission from a seven-ridge laser array versus different phase sector biases. A tuning range of 1.5 GHz out of 3.9 THz ($\sim$0.04%) was observed. This fine and fast (compare to temperature tuning) tunability is desirable for frequency- or phase-locking applications.

In summary, we report the phase-locked array implemented in THz QCLs. The phase-locking is achieved through phase sectors between laser ridges. Up to six laser ridges are locked in-phase with single-lobe far-field beam-pattern (FWHM $\approx 10°$) along the array direction. The laser array can

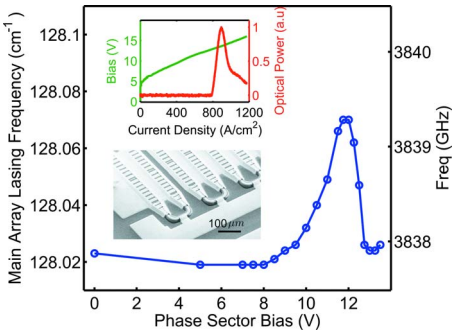

FIG. 4. (Color online) Frequency shift of the emission from a seven-ridge array vs dc biases on the phase sectors. Pulsed L-I-V measurements of main laser ridges (inset) and a closer look of the phase sectors (SEM picture).

be further modified to enable biasing individual lasers and thus control the amplitude of the wave front across laser arrays, obtaining beam-steering capability. Even though the phase-locked arrays are demonstrated with surface-emitting lasers, the same coupling method can be applied to other types of MM waveguide lasers, such as the third-order DFB lasers,[9] for additional functionality.

We would like to thank S. Kumar for helpful discussions and A. W. M. Lee for the THz imaging measurement. This work is supported by AFOSR, NASA, and NSF. Sandia is a multiprogram laboratory operated by Sandia Corporation, a Lockheed Martin Co., for the U.S. Department of Energy under Contract No. DE-AC04-94AL85000.

[1] B. S. Williams, S. Kumar, H. Callebaut, Q. Hu, and J. L. Reno, Appl. Phys. Lett. **83**, 2124 (2003).
[2] S. Kumar, Q. Hu, and J. L. Reno, Appl. Phys. Lett. **94**, 131105 (2009).
[3] A. J. L. Adam, I. Kašalynas, J. N. Hovenier, T. O. Klaassen, J. R. Gao, E. E. Orlova, B. S. Williams, S. Kumar, Q. Hu, and J. L. Reno, Appl. Phys. Lett. **88**, 151105 (2006).
[4] S. Kumar, B. S. Williams, Q. Qin, A. W. M. Lee, Q. Hu, and J. L. Reno, Opt. Express **15**, 113 (2007).
[5] J. Fan, M. Belkin, F. Capasso, S. Khanna, M. Lachab, A. Davies, and E. Linfield, Opt. Express **14**, 11672 (2006).
[6] Y. Chassagneux, R. Colombelli, W. Maineult, S. Barbieri, H. E. Beere, D. A. Ritchie, S. P. Khanna, E. H. Linfield, and A. G. Davies, Nature (London) **457**, 174 (2009).
[7] Y. Chassagneux, R. Colombelli, W. Maineult, S. Barbieri, S. P. Khanna, E. H. Linfield, and A. G. Davies, Appl. Phys. Lett. **96**, 031104 (2010).
[8] W. Maineult, P. Gellie, A. Andronico, P. Filloux, G. Leo, C. Sirtori, S. Barbieri, E. Peytavit, T. Akalin, J. Lampin, H. E. Beere, and D. A. Ritchie, Appl. Phys. Lett. **93**, 183508 (2008).
[9] M. I. Amanti, M. Fischer, G. Scalari, M. Beck, and J. Faist, Nat. Photonics **3**, 586 (2009).
[10] D. E. Ackley, Appl. Phys. Lett. **42**, 152 (1983).
[11] J. Katz, S. Margalit, and A. Yariv, Appl. Phys. Lett. **42**, 554 (1983).
[12] K. L. Chen and S. Wang, Electron. Lett. **21**, 347 (1985).
[13] D. Botez and G. Peterson, Electron. Lett. **24**, 1042 (1988).
[14] D. Botez, L. J. Mawst, G. L. Peterson, and T. J. Roth, IEEE J. Quantum Electron. **26**, 482 (1990).
[15] D. Botez and D. R. Scrifres, *Diode Laser Arrays* (Cambridge University Press, New York, 1994).
[16] S. Kohen, B. S. Williams, and Q. Hu, J. Appl. Phys. **97**, 053106 (2005).
[17] L. K. Hoffmann, C. A. Hurni, S. Schartner, M. Austerer, E. Mujagic, M. Nobile, A. Benz, W. Schrenk, A. M. Andrews, P. Klang, and G. Strasser, Appl. Phys. Lett. **91**, 161106 (2007).
[18] R. K. DeFreez, D. J. Bossert, N. Yu, K. Hartnett, R. A. Elliott, and H. G. Winful, Appl. Phys. Lett. **53**, 2380 (1988).
[19] A. W. M. Lee, Q. Qin, S. Kumar, B. S. Williams, Q. Hu, and J. L. Reno, Appl. Phys. Lett. **89**, 141125 (2006).